CMS Physics Analysis Summary

Contact: cms-pag-conveners-heavyions@cern.ch 2019/11/05

Study of quark- and gluon-like jet fractions using jet charge in PbPb and pp collisions at 5.02 TeV

The CMS Collaboration

Abstract

The momentum-weighted sum of the electric charges of particles inside a jet, known as jet charge, is sensitive to the charge of the particle initiating the parton shower. This note presents jet charge distributions in 5.0 TeV PbPb and pp collisions recorded by the CMS detector at the LHC. These data correspond to integrated luminosities of 404 μb^{-1} and 27.4 pb^{-1} for PbPb and pp collisions, respectively. The measurements are unfolded to account for detector and background effects. Leveraging the jet charge's sensitivity to fundamental differences in the electric charges of quarks and gluons, a template-fitting method is proposed to estimate the quark- and gluon-like jet fractions of an inclusive jet sample. Using the jet charge distributions from simulated events as templates, the quark and gluon jet fractions are extracted from data. The modification of these jet fractions is examined by comparing PbPb and pp data as a function of collision centrality. This measurement tests the color charge dependence of jet energy loss due to interactions with the quark-gluon plasma.

1 Introduction

High-momentum partons produced by hard scatterings in heavy ion collisions are predicted to suffer energy loss as they traverse the quark-gluon plasma (QGP) created in these interactions [1]. The mechanisms by which these partons lose energy to the medium, as well as their color dependence, are still not fully understood [2, 3]. The particles resulting from the fragmentation and hadronization of these partons can be clustered into jets. Jets are used as parton proxies to examine the properties of the QGP. Parton energy loss manifests itself in various experimental observables including the suppression of high transverse momentum (p_{T}) hadrons and jets [4–8] as well as modifications of parton showers [9, 10]. These phenomena are collectively referred to as jet quenching [1].

At leading order in quantum chromodynamics, the type of parton that initiates a jet can be distinguished. The resulting jet can therefore be labeled as a quark jet, an antiquark jet, or a gluon jet. Several recent measurements indicate that the fractions of quark and gluon jets in a sample may be modified because of quenching in the QGP [11, 12]. This analysis explores the extraction of the fractions of quark and gluon jets from an inclusive jet sample in proton-proton (pp) and lead-lead (PbPb) collisions. This is achieved with a template-fitting method using the "jet charge" observable. Jet charge, defined as the momentum-weighted sum of the electric charges of particles inside a jet, is sensitive to the charge of the particle initiating a parton shower and can be used to discriminate between gluon-initiated and quark-initiated jets. This observable was initially suggested by Field and Feynman as a way of measuring the charge of a quark [13]. It was first measured in deep inelastic scattering experiments at Fermilab [14, 15], CERN [16–19], and Cornell [20] in an effort to understand quark and hadron models. A detailed investigation of jet charge and its applications in heavy ion collisions is motivated by recent theoretical calculations [21–23]. The dependence of the average and width of the jet charge on both jet energy and size can be calculated independently of Monte Carlo (MC) fragmentation models despite the large experimental uncertainty on fragmentation functions [24]. Unlike the total particle multiplicity within the jet cone, which is directly affected by jet quenching [25], the jet charge of a given jet is expected to be relatively unmodified in heavy-ion collisions. This makes it a more reliable variable for the determination of quark and gluon fractions via template fitting.

In this note, jet charge measurements are presented for pp and PbPb collisions. The analysis uses data collected at a center-of-mass energy per nucleon pair ($\sqrt{s_{\mathrm{NN}}}$) of 5.02 TeV in 2015, corresponding to integrated luminosities of 404 $\mu\mathrm{b}^{-1}$ for PbPb and 27.4 pb^{-1} for pp. In heavy ion events, where separation of jet and background constituents is not straightforward and often impossible on a per-particle basis, "background" is defined as uncorrelated and long-range correlated contributions [26], as measured at least 1.5 units of relative pseudorapidity away from the jet axis [10, 27, 28]. Any short-range modifications to either the medium or the jet structure are thus included in the (modified) jet. In this analysis, the measurements are unfolded for detector and background effects, and are presented as a function of the overlap of the colliding Pb nuclei (centrality), with head-on collisions defined as most central. The jet charge distributions of quark and gluon jets from MC generators are used as templates to fit the inclusive jet charge distribution measured in data. The fractions of quark- and gluon-initiated jets are extracted from this fitting procedure. The results are presented as a function of the minimum p_{T} threshold of the particles used in the jet charge measurement and also as a function of a p_{T} weighting factor, κ.

2 The CMS detector

The central feature of the CMS apparatus is a superconducting solenoid of 6 m internal diameter, providing a magnetic field of 3.8 T. Within the solenoid volume are a silicon pixel and strip tracker, a lead tungstate crystal electromagnetic calorimeter (ECAL), and a brass and scintillator hadron calorimeter (HCAL), each composed of barrel and endcap sections. Two hadron forward (HF) steel and quartz-fiber calorimeters complement the barrel and endcap detectors, extending the calorimeter from the range $|\eta| < 3.0$ provided by the barrel and endcap out to $|\eta| < 5.2$.

Jets are reconstructed within the range $|\eta| < 1.6$. In the region $|\eta| < 1.74$, the HCAL cells have widths of 0.087 in both η and ϕ. Within the central barrel region of $|\eta| < 1.48$, the HCAL cells map onto 5×5 ECAL crystal arrays to form calorimeter towers projecting radially outwards from the nominal interaction point. Within each tower, the energy deposits in ECAL and HCAL cells are summed to define the calorimeter tower energies, which are subsequently clustered to reconstruct the jet energies and directions [29].

The CMS silicon tracker measures charged-particle tracks within $|\eta| < 2.5$. It consists of 1440 silicon pixel and 15 148 silicon strip detector modules. For charged particles with $1 < p_{\mathrm{T}} < 10$ GeV in the barrel region, the track resolutions are typically 1.5% in p_{T} and 25–90 (45–150) μm in the impact parameter direction transverse (longitudinal) to the colliding beams [30]. A detailed description of the CMS detector, together with a definition of the coordinate system used and the relevant kinematic variables, can be found in Ref. [31].

3 Event selection and simulated event samples

The pp and PbPb data are selected with a calorimeter-based trigger that uses the anti-k_{T} jet clustering algorithm with distance parameter of $R = 0.4$ [32, 33]. The trigger requires events to contain at least one jet with $p_{\mathrm{T}} > 80$ GeV. This trigger is fully efficient for events containing jets with reconstructed $p_{\mathrm{T}} > 100$ GeV. For both PbPb and pp collisions, the data selected by this trigger are referred to as "jet-triggered." Vertex and noise filters are applied to both pp and PbPb data to reduce contamination from non-collision events (beam–gas, beam–pipe, beam–halo, beam–scraping, cosmics and calorimeter noise) as described in previous analyses [34]. Additionally, a primary vertex with at least 2 tracks is required to be present within 15 cm of the center of the nominal interaction region along the beam axis ($|v_z| < 15$ cm). In PbPb collisions, the shapes of the clusters in the pixel detector are required to be compatible with those expected from particles produced by a PbPb collision. The PbPb events are also required to have at least three towers in each of the HF detectors with energy deposits of more than 3 GeV per tower.

Simulated MC samples are used to evaluate the performance of the event reconstruction, particularly the track reconstruction efficiency and the jet energy response and resolution. The MC samples use the PYTHIA (version 6.424, tune Z2 [35, 36]) event generator to describe the hard scattering, parton showering, and hadronization of the partons. To account for the soft underlying PbPb event, the hard PYTHIA interactions are embedded into simulated minimum-bias PbPb events produced with HYDJET 1.383 [37]. This minimum-bias event generator is tuned to reproduce global event properties such as the charged-hadron p_{T} spectrum and particle multiplicity. The combined sample of hard PYTHIA interactions and soft HYDJET underlying event is referred to as PYTHIA + HYDJET. The GEANT4 [38] toolkit is used to simulate the CMS detector response.

The scalar p_T sum of calorimeter towers in the HF region ($3.0 < |\eta| < 5.2$) is used to define the event centrality in PbPb events and to divide the event sample into centrality classes, each representing a percentage of the total nucleus-nucleus hadronic interaction cross section [7]. Events in PbPb collisions are divided into four centrality intervals given by 0–10% (most central, corresponding to the largest overlap of the colliding nuclei), 10–30%, 30–50%, and 50–100% (most peripheral).

Because of the large number of binary nucleon-nucleon collisions in central events, requiring a jet to be present in an event biases the data sample towards more central collisions. In comparison, the PYTHIA + HYDJET sample consists of a flat distribution of jets (from PYTHIA) as a function of centrality, embedded in simulated minimum-bias PbPb collisions. Thus, a centrality-based reweighting is applied to this MC sample to match the centrality distribution of the jet-triggered PbPb data. An additional reweighting procedure is performed to match the simulated v_z distributions to data for both the pp and PbPb samples.

4 Jet and track reconstruction

The offline jet reconstruction in PbPb and pp events is performed with the anti-k_T jet algorithm having a distance parameter of $R = 0.4$, as implemented in the FASTJET framework [39]. Individually calibrated calorimeter towers are used as inputs to the algorithm. Only calorimeter information is used in the jet reconstruction to ensure that the tracking efficiency does not bias the reconstruction of jets. In PbPb collisions, the contributions of the underlying event are subtracted using a two-iteration variant of the "noise/pedestal subtraction" technique described in Ref. [40, 41]. In this method, only calorimeter towers outside of the jet area are used in the background estimation after identifying and excluding the jets in the first iteration. Following this subtraction, jets are calibrated such that the calorimeter response is uniform as a function of jet p_T and η. To account for the variation in detector response with the total number of jet constituents, additional corrections are applied based on the number of charged-particle tracks with $p_T > 2$ GeV within the jet cone, the jet p_T and collision centrality. This corrects for a difference in the simulated calorimetric jet energy response between quark and gluon jets and reduces the difference in response between the two jet flavors from 10% to around 3%. After reconstruction and offline jet energy calibration, jets are required to have $p_T > 120$ GeV and $|\eta| < 1.5$. Within this selection, it is possible for multiple jets to be selected from the same event. Roughly 25% of pp events contain multiple jets that satisfy all kinematic selection criteria.

For pp data and simulations, charged-particle tracks are reconstructed using an iterative tracking method [30] that finds tracks within $|\eta| < 2.4$ down to $p_T = 0.1$ GeV. For the PbPb data an alternative iterative reconstruction procedure is employed because of the large track multiplicities [42, 43]. It is capable of reconstructing tracks down to $p_T = 0.4$ GeV. Tracks used in this measurement are required to have a relative p_T uncertainty of less than 10% (30%) in PbPb (pp) collisions and also satisfy the standard track quality cuts [34]. In PbPb collisions, tracks must have at least 11 hits and satisfy a fit quality requirement that the χ^2, divided by both the number of degrees of freedom and the number of tracker layers hit, be less than 0.15. For both collision systems, a selection requirement of less than 3 standard deviations is applied on the significance of the distance of closest approach to at least one primary vertex in the event to decrease the likelihood of counting nonprimary charged particles originating from secondary decay products. Tracks with $p_T > 20$ GeV are required to have an associated energy deposit [44] of at least half their momentum in the calorimeters to reduce the contribution of misreconstructed tracks with very high p_T. The tracking efficiency in pp collisions is approximately 90% for $p_T > 1$ GeV. Track reconstruction is more difficult in the heavy ion environment

because of the large track multiplicity, and so the tracking efficiency ranges from approximately 60% at $p_{\mathrm{T}} = 1\,\mathrm{GeV}$ to about 70% at $p_{\mathrm{T}} = 10\,\mathrm{GeV}$ [34].

5 Jet charge measurements

Jet charge refers to the p_{T}-weighted sum of the electric charges of the particles in a jet [13]. It is defined as:

$$Q^{\kappa} = \frac{1}{(p_{\mathrm{T}}^{\mathrm{jet}})^{\kappa}} \sum_{i \in jet} q_i (p_{\mathrm{T}}^{i})^{\kappa}. \tag{1}$$

The variable $p_{\mathrm{T}}^{\mathrm{jet}}$ is the transverse momentum of the calorimeter jet, q_i is the charge of the particle, and p_{T}^{i} is the magnitude of the transverse momentum of the particle relative to the beam axis. The κ parameter controls the sensitivity of the jet charge variable to low and high p_{T} particles in the jet cone. Low values of κ enhance the contribution from low p_{T} particles to the jet charge and vice versa.

Tracks with $p_{\mathrm{T}} > 1\,\mathrm{GeV}$ that are located within the jet cone (relative angular distance from the jet axis $\Delta \mathrm{r} = \sqrt{(\Delta\eta)^2 + (\Delta\phi)^2} < 0.4$) are used in the jet charge measurement. The track p_{T} cutoff of 1 GeV ensures that the MC templates for different flavors used in the fitting procedure are well resolved and also reduces the contributions of combinatorial and long-range correlated background to the jet charge. Theoretical predictions suggest that $\kappa \sim 0.5$ is the most sensitive to the charge of the parton initiating a jet [21]. In this analysis, measurements are shown for κ values of 0.3, 0.5 and 0.7, and with different cuts on the track p_{T} of 1, 2, 4, and 5 GeV to maintain a broad sensitivity to both hard and soft radiation inside jets.

6 Unfolding of background and detector effects

To compare with measurements from other experiments or theoretical predictions, the jet charge distributions are unfolded from the detector-level to the final-state particle level. The jet charge measurements at the detector-level are smeared by track reconstruction inefficiencies, and this effect increases with decreasing κ values. In PbPb collisions, there is additional smearing that is caused by the background from the underlying event and long-range correlations, e.g., azimuthal anisotropies [26]. Unfolding is performed to account for these effects using D'Agostini's iteration method with early stopping [45–47], as implemented in the RooUnfold software package [48]. Response matrices are derived from PYTHIA for pp and from PYTHIA + HYDJET for PbPb collisions. The unfolding procedure used here is a two step process.

In the first step, the distributions in PbPb collisions are unfolded at the detector-level to account for the background effects. For this purpose, response matrices are populated using the jet charge measured with reconstructed tracks coming from both the hard scattering and the background. These values are mapped onto measurements only using tracks originating from the hard scattering. As a cross check of this procedure, the unfolding matrices are also built using a data-driven event mixing technique to estimate the long-range correlated and uncorrelated background contributions. The jet charge is measured using jet-track pairs built from jets in a jet-triggered event and tracks from a separate minimum-bias event. These two events are required to have a v_z within 1 cm of each other and a collision centrality within 2.5%. The data-driven background is observed to be in close agreement with HYDJET.

After unfolding for background effects, the jet charge distributions are then unfolded for tracking inefficiencies using response matrices constructed with reconstructed tracks and generator-level particles only originating from the hard scattering. To obtain an optimal number of iterations for the unfolding procedure, reconstructed jet charge distributions from a modified sample of PYTHIA, with the quark and gluon jet fractions varied by 50%, is unfolded using the nominal response matrices. Based on these studies, it is observed that three or four iterations, for different selections of threshold track p_T and κ, is optimal in balancing the bias towards the MC distribution with increasing statistical fluctuations. The systematic uncertainties in the unfolding procedure are discussed in Sec. 8.

7 Template fitting

The flavor-tagged jet charge distributions from generator-level PYTHIA and PYTHIA + HYDJET are used as templates in fitting the unfolded jet charge measurement to estimate the fractions of quark and gluon jets. Measurements from PYTHIA simulations for jets initiated by up quarks (mean $= 0.288e$), down quarks (mean $= -0.165e$) and gluons (mean $= 0.001e$) are well resolved and make up the dominant proportions of the sample. The means for different flavor jets reported here are from measurements at the generator-level, with a track p_T cut-off of 2 GeV and κ value of 0.5. They have statistical uncertainties of less than 0.1%. The average jet charge for jets initiated by quarks and gluons varies by less than 1% as a function of the jet p_T in PYTHIA, allowing the stable extraction of the respective jet fractions in the p_T range examined here. Transverse momentum spectra of different flavor jets and their fractions are studied from PYTHIA and PYTHIA +HYDJET, and an enhancement of the up and down quark jet fractions is observed with increasing jet p_T. The relative fractions of heavy quark (c, s and b) jets are fixed during the fitting procedure. The systematic uncertainty related to this assumption is estimated by varying the heavy quark jets by their total fraction and studying the effects on the fitting results. The fitting procedure takes into consideration the total systematic uncertainties on the jet charge measurements from all sources added in quadrature to the statistical uncertainties.

A small fraction of jets have no tracks inside the jet cone above the threshold track p_T used in the jet charge measurement. For a track p_T cut of 5 GeV, this fraction goes up to 6% in pp collisions and 10% in central PbPb collisions. The fraction of such jets is negligible in both pp and PbPb collisions for a track p_T cut of 1 GeV. Such jets are excluded in the fitting procedure, and the relative fractions of quarks and gluons for such jets are assigned directly from MC. Previous CMS results have shown a large excess of soft particles in PbPb events relative to pp events up to $\Delta r \sim 1$ from the jet axis, compensated by a relative depletion of high p_T tracks [10, 49]. As a result, the fraction of jets consisting of no tracks with $p_T > 4$ GeV is observed to be higher in PbPb data than PYTHIA + HYDJET, and this difference increases as the collisions become more central.

For a given jet energy, jets with a harder constituent p_T spectrum are more likely to be successfully reconstructed because the calorimeter response does not scale linearly with incident particle energy, resulting in a bias toward the selection of jets with fewer associated tracks. On average, quark jets have a harder fragmentation than gluon jets and are therefore preferentially reconstructed. Jet energy corrections based on the number of jet constituents are applied (Sec. 4) to reduce the difference in the response between quark and gluon jets from 10% to around 3%. To compensate for this residual difference in response, an extra correction factor is applied to the extracted fractions of quark and gluon jets.

8 Systematic uncertainties

A number of sources of systematic uncertainty are considered, including effects from unfolding, tracking efficiencies, background correction, jet reconstruction and the contributions from heavy quarks and antiquarks. The systematic uncertainties from all sources are added in quadrature. The relative uncertainties on the measured jet charge distributions vary for different selections of κ and track p_{T} threshold.

The difference in tracking efficiencies for positive and negative particles is found to be 0.5% regardless of the particle p_{T}. The relative reconstruction efficiency between positively-charged and negatively-charged tracks is varied by this amount when populating the response matrices used in the data unfolding. The resulting jet charge distributions are fit with the generator-level templates and the differences in the extracted fractions of quarks and gluons are cited as a source of systematic uncertainty.

An uncertainty of 4% in pp and 5% in PbPb is evaluated to account for possible differences in track reconstruction between data and simulation, including erroneous reconstruction of tracks. This uncertainty is propagated to the final result in a fashion similar to what is used for the relative tracking uncertainty between positive and negative particles, i.e., the unfolding response matrices are modified and any differences after applying the template fitting procedure are taken as systematic uncertainties. Based on these tracking studies an uncertainty of 1–2% is assigned to the extracted jet fractions.

To study the systematic effect arising from the choice of the PYTHIA generator to produce the response matrix used in the unfolding procedure, a response matrix is formed using a modified PYTHIA sample with varied quark and gluon jet fractions, and both of these matrices are used to unfold the data. The corresponding difference in the unfolded distributions is taken as the uncertainty in the modeling of the response matrix. In this study, quark and gluon jet fractions are varied by 50% from their nominal MC values while populating the modified response matrices resulting in a relative uncertainty of 4–7% on the extracted jet fractions. Other uncertainties in the unfolding procedure include effects from statistical uncertainty in the MC simulation of the matrix elements in the response matrix and the uncertainty propagated via bin-to-bin correlations as a result of the regularization process. They are propagated using the RooUnfold software package.

The systematic uncertainty due to the jet energy resolution is estimated by changing the jet energy resolution by 5% to cover the uncertainty in these quantities [50], followed by a comparison of the modified spectra with the nominal spectrum. The corresponding differences in the extracted quark and gluon fractions are 1–3% and are included as systematic uncertainties. The effects of the angular resolution of the jet axis are negligible in the jet charge measurements.

To study the background modeling uncertainty, the contribution from the background is alternatively estimated using a data-driven event mixing technique. The jet charge is measured by pairing the reconstructed jet from a signal event to tracks from an event in a minimum bias data sample. The minimum-bias event is selected to have a similar vertex position (v_z within 1 cm) and event centrality (within 2.5%) to the jet event. The data-driven background is in close agreement with HYDJET resulting in uncertainty values of less than 1%.

The contribution from jets with zero tracks in the jet cone above the threshold p_{T} cut, which are excluded in the fitting procedure, to the quark/gluon ratio measurements is assigned from MC. The difference in the fraction of such jets between data and MC increases with increasing track p_{T} cut and with more central collisions because of the observed depletion of high p_{T} tracks in PbPb collisions [10, 49]. This difference is less than 1% in pp collisions but can reach 4.5% in

PbPb collisions. It is assigned as a systematic uncertainty.

In PbPb data, there is an additional jet reconstruction bias toward selecting jets that sit on upward fluctuations in the underlying event. Since the jet spectrum is steeply falling, more jets on upward fluctuations are included in the sample than jets on downward fluctuations are excluded. This effect is expected to be included in the reconstructed jet charge measurements in MC as well and so the difference in this bias between data and MC is used to calculate the corresponding systematic uncertainty. To calculate this difference, particle multiplicity distributions in cones ($R = 0.4$), chosen randomly in detector pseudorapidity and azimuth, are compared between minimum bias data and MC events. The difference is then propagated as a source of systematic uncertainty and is observed to be negligible.

To assess the effects of the statistical uncertainties from the MC templates on the final results, 1000 pseudo-experiments are performed by generating smeared jet charge templates based on its statistical uncertainty and repeatedly fitting the data measurements using these templates. The distributions of extracted gluon jet fractions from the pseudo-experiment fits have a variance of 3% or less, which is assigned as a systematic uncertainty due to limited MC statistics. The uncertainty on the fit results due to the choice of the jet charge distribution binning is a minor effect and is included as a systematic uncertainty.

Finally, the effect of fixing the heavy quark jet fractions in the fitting procedure is analyzed. The heavy quark jets are each independently varied by their full fraction and the effects of this on the fit results are observed to be small compared to the other systematic uncertainties. A summary of the range of systematic uncertainties for results is shown in Table 1 for different selections of κ and track p_{T} threshold values.

Table 1: Relative systematic uncertainties in percentage for the measurements of gluon-like jet fractions in PbPb and pp events. The PbPb results are given in intervals of centrality. When an uncertainty range is given, the range of the values are the maximum variation in the relative fractions for different selections of κ and track p_{T} threshold values.

	PbPb centrality intervals				pp
Source	0–10%	10–30%	30–50%	50–100%	
Response matrix modeling	5–7.5	5–7.5	5–7.5	5–7.5	4–6
Monte Carlo statistics	3	3	3	3	1.5
Jet energy resolution	2–3	2–3	2	2	1–1.5
Tracking efficiency (data/MC)	2	2	2	2	1
Tracking efficiency (positive/negative)	0.5–1.5	0.5–1.5	1–1.5	1–1.5	0.5–1
Zero track jets	0.5–4.5	0.4–3	0.4–2	0.2–1	0.1
Unfolding procedure	1.4	1.1	0.8	0.7	0.5
Background modeling and fluctuation	1	1	0.5	0.5	—
Heavy flavor jets	1	1	1	1	1
Total	7–9	7–8	7–8	7–8	4–5

9 Results

The unfolded jet charge measurements, normalized to the total number of jets in the sample, are shown in the top panel of Fig. 1 with solid black points for a sample bin with a minimum track p_{T} of 1 GeV and $\kappa = 0.5$. The results are shown for pp and different event centrality bins in PbPb. The extracted fraction of light quark and gluon-initiated jets is displayed as a set of stacked histograms. The heavy quark and antiquark jet contribution is labeled as "other flavors." Figure 1 also shows the ratio of the data over the template fit results in the bottom panel,

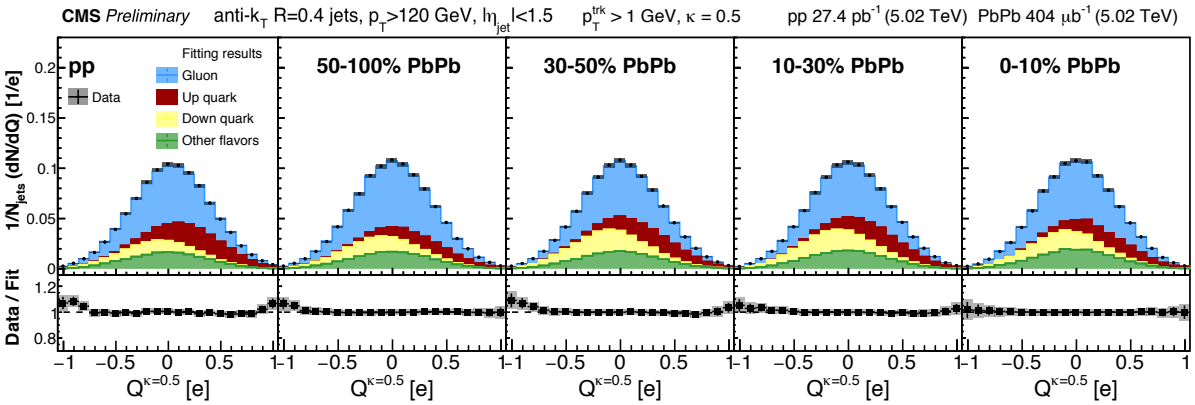

Figure 1: (Top) Unfolded jet charge measurements shown for inclusive jets in data along with the extracted fractions of up and down quark jets, gluon jets, and the heavy and antiquark jets (collectively grouped as "other flavors"). The systematic uncertainties on the distributions are shown in shaded regions around the measurements. The jet charge measurements shown here are for $\kappa = 0.5$ and a minimum track p_T of 1 GeV. (Bottom) Ratio of the jet charge measurements to the results of template fits.

which is observed to be relatively flat in the entire fitting range. The jet charge measurements and fit results for other minimum track p_T and κ selections are shown in the Appendix.

The widths of the unfolded data jet charge distributions with different track p_T cuts and κ values are compared to generator-level measurements from PYTHIA in Fig. 2 in different centrality bins. The results for κ = 0.3, 0.5, and 0.7, are shown by the blue, red, and green points, respectively. The measurement in data is shown by the open boxes, and for PYTHIA is shown by the open crosses. The measured standard deviations tend to increase as a function of the minimum track p_T and decrease with increasing κ. Theoretical predictions incorporating color-charge dependence into jet energy loss calculations expect that stronger quenching of gluon jets will result in a reduced fraction of gluon-initiated jets in the observed jet sample from PbPb collisions compared to that in pp [22]. The mean of the jet charge distribution for gluon-initiated jets is consistently predicted to be zero in various MC simulations, while that of quark jets is nonzero. A decrease in the fraction of gluons in a quenched jet sample would hence lead to an effective increase in the standard deviation of the measured jet charge distribution. Figure 2 summarizes standard deviations measured for all track p_T selections and κ values studied. The PYTHIA predictions agree with the measured widths for pp events. No strong modifications are observed in the widths of the jet charge distributions in central PbPb collisions compared to the peripheral events. While the PbPb width results cannot be directly compared to the pp reference due to different up and down quark content in protons and Pb nuclei, PYTHIA predictions adjusted for this difference reproduce the observed widths of jet charge measurements for all PbPb collision centralities.

The consolidated results for the quark and gluon jet fractions in an inclusive sample are shown in Fig. 3 as a function of the minimum track p_T. Figure 4 shows the same quantities as a function of κ for track $p_T > 1$ GeV and track $p_T > 2$ GeV, with red and blue points respectively. The systematic uncertainties are shown in shaded regions and the statistical uncertainties, along with the fit uncertainties, are shown in solid vertical bars. Previous CMS measurements have shown a strong modification in the distribution of low p_T tracks relative to the jet axis in PbPb collisions with respect to pp collisions [10, 49]. In-medium gluon radiation and a wake-like response of the QGP to the propagating parton are two of the proposed explanations for this

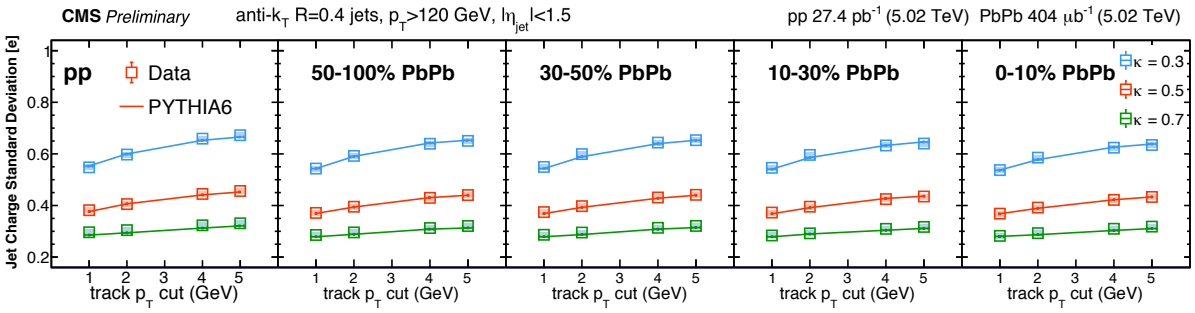

Figure 2: The standard deviation of the jet charge distributions with different track p_T cuts and κ values for pp collisions and in the various event centrality bins for PbPb collisions compared with PYTHIA + HYDJET.

modification, neither of which are expected to modify the jet charge considerably. From Fig. 3 and Fig. 4, no significant modification is observed in the relative fractions of the quark and gluon jets in central PbPb collisions compared to peripheral PbPb and pp collisions. The relative jet fractions are also observed to be unmodified when calculated using a range of different track p_T cuts or κ values.

10 Summary

The first measurements of jet charge in PbPb collisions using data collected with the CMS detector at a nucleon-nucleon center-of-mass energy of $\sqrt{s_{NN}} = 5.02$ TeV are presented. Measurements in pp collisions at the same energy are also reported. The unfolded jet charge distributions, measured using the jet constituents with transverse momentum $p_T > 1$ GeV for jets having $p_T > 120$ GeV and $|\eta| < 1.5$, are presented. The width of the jet charge distributions for pp collisions and in different event centrality bins for PbPb collisions are shown to be independent of collision centrality and are in good agreement with measurements from PYTHIA and PYTHIA + HYDJET. The jet charge distributions for quark- and gluon-initiated jets from PYTHIA and PYTHIA + HYDJET are used as fitting templates to estimate the respective contributions in the measured jet samples. The gluon-like jet fractions extracted from these template fits are found to be similar between pp and all studied PbPb centrality ranges. No evidence is seen for a significant decrease in gluon prevalence due to jet quenching in PbPb collisions in the sample

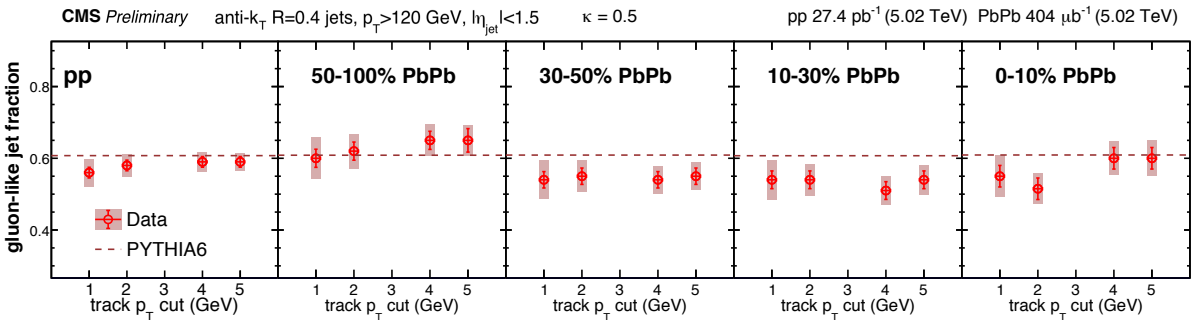

Figure 3: Fitting results for the extraction of gluon-like jet fractions in pp and PbPb data shown for different minimum track p_T values and for different event centrality bins in PbPb. The systematic uncertainties are shown by shaded regions and the statistical uncertainties are shown by vertical bars.

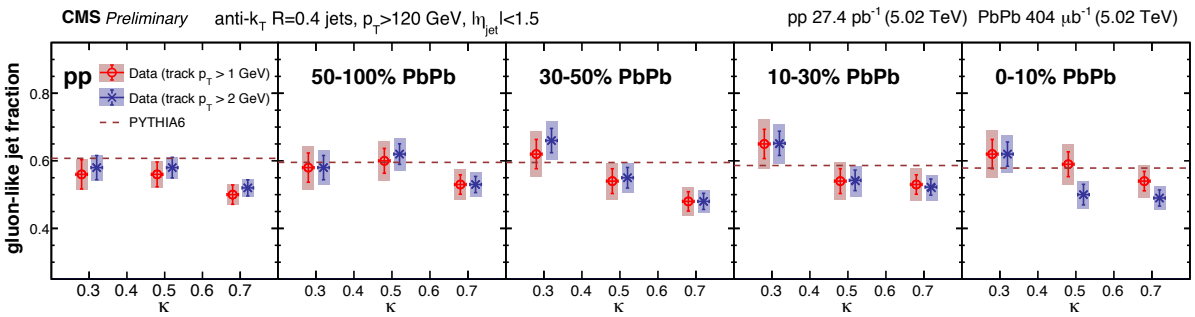

Figure 4: Fitting results for the extraction of gluon-like jet fractions in pp and PbPb data shown for κ values of 0.3, 0.5 and 0.7 in different event centrality bins in PbPb. The markers for track $p_{\mathrm{T}} > 1$ GeV and track $p_{\mathrm{T}} > 2$ GeV have been separated horizontally for clarity. The systematic uncertainties are shown by shaded regions and the statistical uncertainties are shown by vertical bars.

of inclusive jets with $p_{\mathrm{T}} > 120$ GeV, contrary to expectations of some jet quenching models.

References

[1] J. D. Björken, "Energy loss of energetic partons in QGP: possible extinction of high p_T jets in hadron-hadron collisions", (1982). FERMILAB-PUB-82-059-THY.

[2] J. C.-S. . C. A. Salgado, "Introductory lectures on jet quenching in heavy ion collisions", in *Theoretical physics. Proceedings, 47th Cracow School, Zakopane, Poland, June 14-22, 2007*, p. 3661. 2007. arXiv:0712.3443.

[3] A. Majumder and M. Van Leeuwen, "The Theory and Phenomenology of Perturbative QCD Based Jet Quenching", *Prog. Part. Nucl. Phys.* **66** (2011) 41, doi:10.1016/j.ppnp.2010.09.001, arXiv:1002.2206.

[4] STAR Collaboration, "Direct observation of dijets in central Au+Au collisions at $\sqrt{s_{NN}}$ = 200 GeV", *Phys. Rev. Lett.* **97** (2006) 162301, doi:10.1103/PhysRevLett.97.162301, arXiv:nucl-ex/0604018.

[5] ATLAS Collaboration, "Observation of a centrality-dependent dijet asymmetry in Lead-Lead collisions at $\sqrt{s_{NN}} = 2.76$ TeV with the ATLAS detector at the LHC", *Phys. Rev. Lett.* **105** (2010) 252303, doi:10.1103/PhysRevLett.105.252303, arXiv:1011.6182.

[6] CMS Collaboration, "Observation and studies of jet quenching in PbPb collisions at $\sqrt{s_{NN}}$ = 2.76 TeV", *Phys. Rev. C* **84** (2011) 024906, doi:10.1103/PhysRevC.84.024906, arXiv:1102.1957.

[7] CMS Collaboration, "Jet momentum dependence of jet quenching in PbPb collisions at $\sqrt{s_{NN}} = 2.76$ TeV", *Phys. Lett. B* **712** (2012) 176, doi:10.1016/j.physletb.2012.04.058, arXiv:1202.5022.

[8] ALICE Collaboration, "Measurement of jet suppression in central Pb-Pb collisions at $\sqrt{s_{NN}}$ = 2.76 TeV", *Phys. Lett. B* **746** (2015) 1, doi:10.1016/j.physletb.2015.04.039, arXiv:1502.01689.

[9] PHENIX Collaboration, "Transverse momentum and centrality dependence of dihadron correlations in Au+Au collisions at $\sqrt{s_{NN}}$ = 200 GeV: Jet-quenching and the response of partonic matter", *Phys. Rev. C* **77** (2008) 011901, doi:10.1103/PhysRevC.77.011901, arXiv:0705.3238.

[10] CMS Collaboration, "Jet properties in PbPb and pp collisions at $\sqrt{s_{NN}}$=5.02 TeV", *JHEP* **06** (2018) 124151, doi:10.1007/JHEP05(2018)006, arXiv:1803.00042.

[11] M. Spousta and B. Cole, "Interpreting single jet measurements in Pb+Pb collisions at the LHC", *EPJC* **76** (2016), no. 2, 50, doi:10.1140/epjc/s10052-016-3896-0.

[12] ALICE Collaboration, "Exploration of jet substructure using iterative declustering in pp and Pb-Pb collisions at LHC energies", (2019). arXiv:1905.02512. Submitted to *Phys. Rev. Lett.*

[13] R. D. Field and R. P. Feynman, "A parametrization of the properties of quark jets", *Nucl. Phys. B.* **136** (1978) 76, doi:10.1016/0550-3213(78)90015-9.

[14] Fermilab–Serpukhov–Moscow–Michigan Collaboration, "Net charge in deep inelastic antineutrino-nucleon scattering", *Phys. Lett. B* **91** (1980) 311, doi:10.1016/0370-2693(80)90456-6.

[15] Fermilab–Serpukhov–Moscow–Michigan Collaboration, "Quark jets from antineutrino interactions (I). net charge and factorization in the quark jets", *Nucl. Phys. B* **184** (1981) 13, doi:10.1016/0550-3213(81)90207-8.

[16] Aachen–Bonn–CERN–Munich–Oxford Collaboration, "Multiplicity distributions in neutrino-hydrogen interactions", *Nucl. Phys. B* **181** (1981) 385, doi:10.1016/0550-3213(81)90532-0.

[17] Aachen–Bonn–CERN–Munich–Oxford Collaboration, "Charge properties of the hadronic system in νp and $\overline{\nu} p$ interactions", *Phys. Lett. B* **112** (1982) 88, doi:10.1016/0370-2693(82)90912-1.

[18] European Muon Collaboration, "Quark charge retention in final state hadrons from deep inelastic muon scattering", *Phys. Lett. B* **144** (1984) 302, doi:10.1016/0370-2693(84)91825-2.

[19] Amsterdam–Bologna–Padua–Pisa–Saclay–Turin Collaboration, "Charged hadron multiplicities in high-energy $\overline{\nu}_\mu n$ and $\overline{\nu}_\mu p$ interactions", *Z. Phys. C* **11** (1982) 283, doi:10.1007/BF01578279. [Erratum: doi:10.1007/BF01571828].

[20] R. Erickson et al., "Charge retention in deep-inelastic electroproduction", *Phys. Rev. Lett.* **42** (1979) 822, doi:10.1103/PhysRevLett.42.822. [Erratum: doi:10.1103/PhysRevLett.42.1246].

[21] W. J. Waalewijn, "Calculating the charge of a jet", *Phys. Rev. D* **86** (2012) 094030, doi:10.1103/PhysRevD.86.094030, arXiv:1209.3019.

[22] S.-Y. Chen, B.-W. Zhang, and E.-K. Wang, "Jet charge in high energy nuclear collisions", arXiv:1908.01518.

[23] H. T. Li and I. Vitev, "Jet charge modification in dense QCD matter", arXiv:1908.06979.

[24] D. Krohn, M. D. Schwartz, T. Lin, and W. J. Waalewijn, "Jet charge at the LHC", *Phys. Rev. Lett.* **110** (2013) 212001, doi:10.1103/PhysRevLett.110.212001, arXiv:1209.2421.

[25] CMS Collaboration, "Measurement of jet fragmentation in PbPb and pp collisions at $\sqrt{s_{\rm NN}} = 2.76$ TeV", *Phys. Rev. C* **90** (2014) 024908, doi:10.1103/PhysRevC.90.024908, arXiv:1406.0932.

[26] CMS Collaboration, "Long-range and short-range dihadron angular correlations in central PbPb collisions at $\sqrt{s_{\rm NN}}$=2.76 TeV", *JHEP* **11** (2011), no. 7, 76, doi:10.1007/JHEP07(2011)076, arXiv:1105.2438.

[27] CMS Collaboration, "Decomposing transverse momentum balance contributions for quenched jets in PbPb collisions at $\sqrt{s_{\rm NN}}$=2.76 TeV", *JHEP* **16** (2016), no. 11, 55, doi:10.1007/JHEP11(2016)055, arXiv:1609.02466.

[28] CMS Collaboration, "Correlations between jets and charged particles in PbPb and pp collisions at $\sqrt{s_{\rm NN}}$=2.76 TeV", *JHEP* **16** (2016), no. 2, 156, doi:10.1007/JHEP02(2016)156, arXiv:1601.00079.

[29] CMS Collaboration, "Determination of jet energy calibration and transverse momentum resolution in CMS", *JINST* **6** (2011) P11002, doi:10.1088/1748-0221/6/11/P11002, arXiv:1107.4277.

[30] CMS Collaboration, "Description and performance of track and primary-vertex reconstruction with the CMS tracker", *JINST* **9** (2014) P10009, doi:10.1088/1748-0221/9/10/P10009, arXiv:1405.6569.

[31] CMS Collaboration, "The CMS experiment at the CERN LHC", *JINST* **3** (2008) S08004, doi:10.1088/1748-0221/3/08/S08004.

[32] M. Cacciari, G. P. Salam, and G. Soyez, "The anti-k_T jet clustering algorithm", *JHEP* **04** (2008) 063, doi:10.1088/1126-6708/2008/04/063, arXiv:0802.1189.

[33] CMS Collaboration, "The CMS trigger system", *JINST* **12** (2017), no. 01, P01020, doi:10.1088/1748-0221/12/01/P01020, arXiv:1609.02366.

[34] CMS Collaboration, "Charged particle nuclear modification factors in PbPb and pPb collisions at $\sqrt{s_{NN}} = 5.02$ TeV", *JHEP* **04** (2017) 039, doi:10.1007/JHEP04(2017)039, arXiv:1611.01664.

[35] T. Sjöstrand, S. Mrenna, and P. Skands, "PYTHIA 6.4 physics and manual", *JHEP* **05** (2006) 026, doi:10.1088/1126-6708/2006/05/026, arXiv:hep-ph/0603175.

[36] R. Field, "Early LHC underlying event data—findings and surprises", in *Hadron collider physics. Proceedings, 22nd Conference, HCP 2010, Toronto, Canada.* 2010. arXiv:1010.3558.

[37] I. P. Lokhtin and A. M. Snigirev, "A model of jet quenching in ultrarelativistic heavy ion collisions and high-p_T hadron spectra at RHIC", *EPJC* **45** (2006) 211, doi:10.1140/epjc/s2005-02426-3, arXiv:hep-ph/0506189.

[38] GEANT4 Collaboration, "GEANT4—a simulation toolkit", *Nucl. Instrum. Meth. A* **506** (2003) 250, doi:10.1016/S0168-9002(03)01368-8.

[39] M. Cacciari, G. P. Salam, and G. Soyez, "FastJet user manual", *EPJC* **72** (2012) 1896, doi:10.1140/epjc/s10052-012-1896-2, arXiv:1111.6097.

[40] M. Cacciari and G. P. Salam, "Pileup subtraction using jet areas", *Phys. Lett. B* **659** (2008) 119, doi:10.1016/j.physletb.2007.09.077, arXiv:0707.1378.

[41] O. Kodolova, I. Vardanian, A. Nikitenko, and A. Oulianov, "The performance of the jet identification and reconstruction in heavy ions collisions with CMS detector", *EPJC* **50** (2007) 117, doi:10.1140/epjc/s10052-007-0223-9.

[42] CMS Collaboration, "Study of high-p_T charged particle suppression in PbPb compared to pp collisions at $\sqrt{s_{NN}}$ = 2.76 TeV", *EPJC* **72** (2012) 1945, doi:10.1140/epjc/s10052-012-1945-x, arXiv:1202.2554.

[43] CMS Collaboration, "Modification of jet shapes in PbPb collisions at $\sqrt{s_{NN}} = 2.76$ TeV", *Phys. Lett. B* **730** (2014) 243, doi:10.1016/j.physletb.2014.01.042, arXiv:1310.0878.

[44] CMS Collaboration, "Particle-flow reconstruction and global event description with the CMS detector", *Journal of Instrumentation* **12** (oct, 2017) P10003, doi:10.1088/1748-0221/12/10/p10003.

[45] G. D'Agostini, "A multidimensional unfolding method based on Bayes' theorem", *Nucl. Instrum. Meth. A* **362** (1995) 487, doi:10.1016/0168-9002(95)00274-X.

[46] W. H. Richardson, "Bayesian-based iterative method of image restoration", *Opt. Soc. Am.* **62** (1972) 55, doi:10.1364/JOSA.62.000055.

[47] L. B. Lucy, "An iterative technique for the rectification of observed distributions", *Astron. J.* **79** (1974) 745, doi:10.1086/111605.

[48] T. Adye, "Unfolding algorithms and tests using RooUnfold", in *Proceedings of the PHYSTAT 2011 Workshop, CERN, Geneva, Switzerland, January 2011, CERN-2011-006*, p. 313. 2011. arXiv:1105.1160.

[49] CMS Collaboration, "Measurement of transverse momentum relative to dijet systems in PbPb and pp collisions at $\sqrt{s_{\mathrm{NN}}} = 2.76$ TeV", *JHEP* **01** (2016) 6, doi:10.1007/JHEP01(2016)006, arXiv:1509.09029.

[50] CMS Collaboration, "Determination of jet energy calibration and transverse momentum resolution in CMS", *Journal of Instrumentation* **06** (2011) P11002, doi:10.1088/1748-0221/6/11/p11002.

11 Appendix

11.1 Jet charge measurements

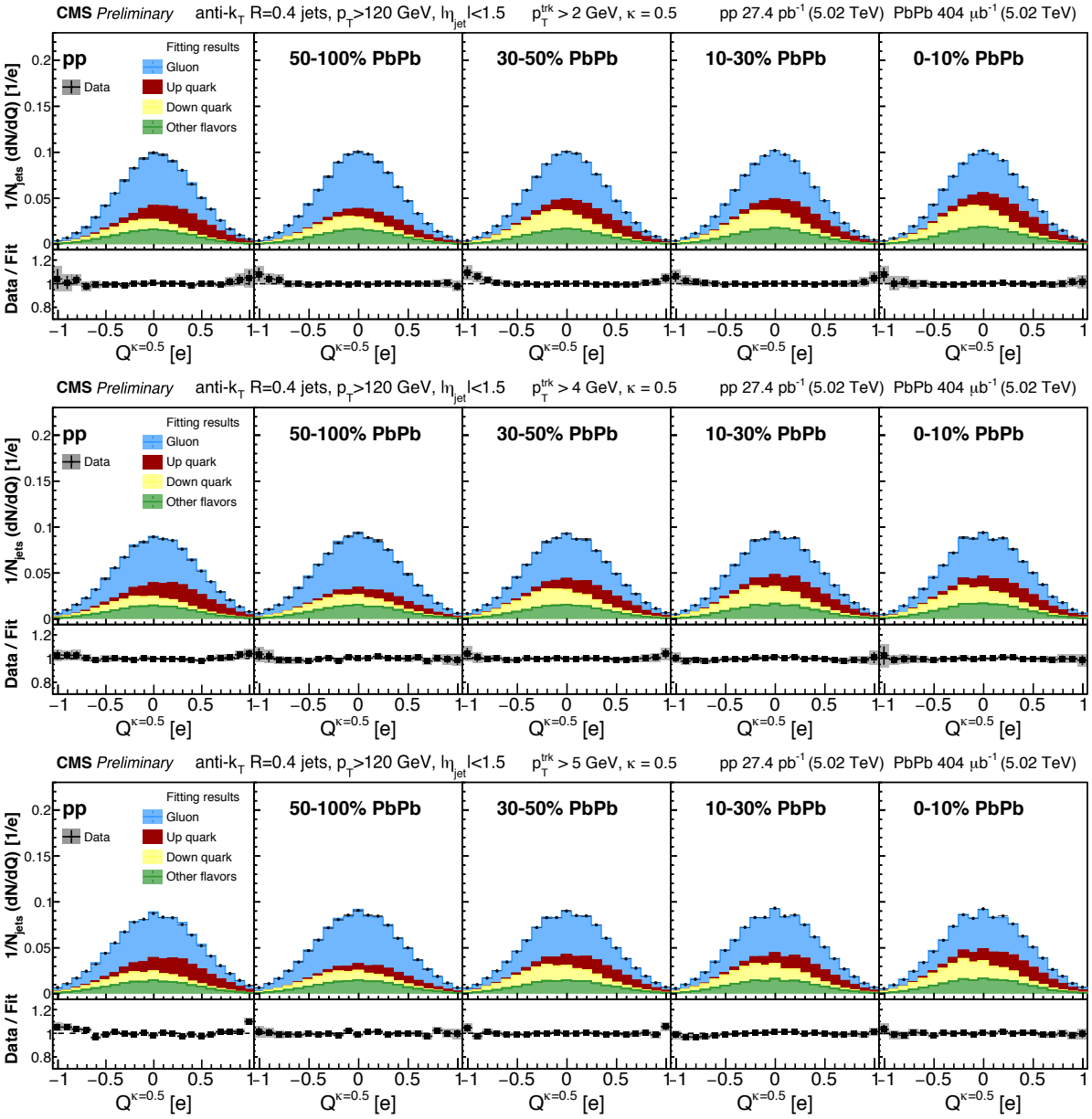

Figure 5: (Top) Unfolded jet charge measurements shown for inclusive jets in data along with the extracted fractions of up and down quark jets, gluon jets, and the heavy and antiquark jets (collectively grouped as "other flavors"). The systematic uncertainties on the distributions are shown in shaded regions around the measurements. The jet charge measurements shown here are for $\kappa = 0.5$ and a minimum track p_T of 2 GeV, 4 GeV and 5 GeV. (Bottom) Ratio of the jet charge measurements to the results of template fits.

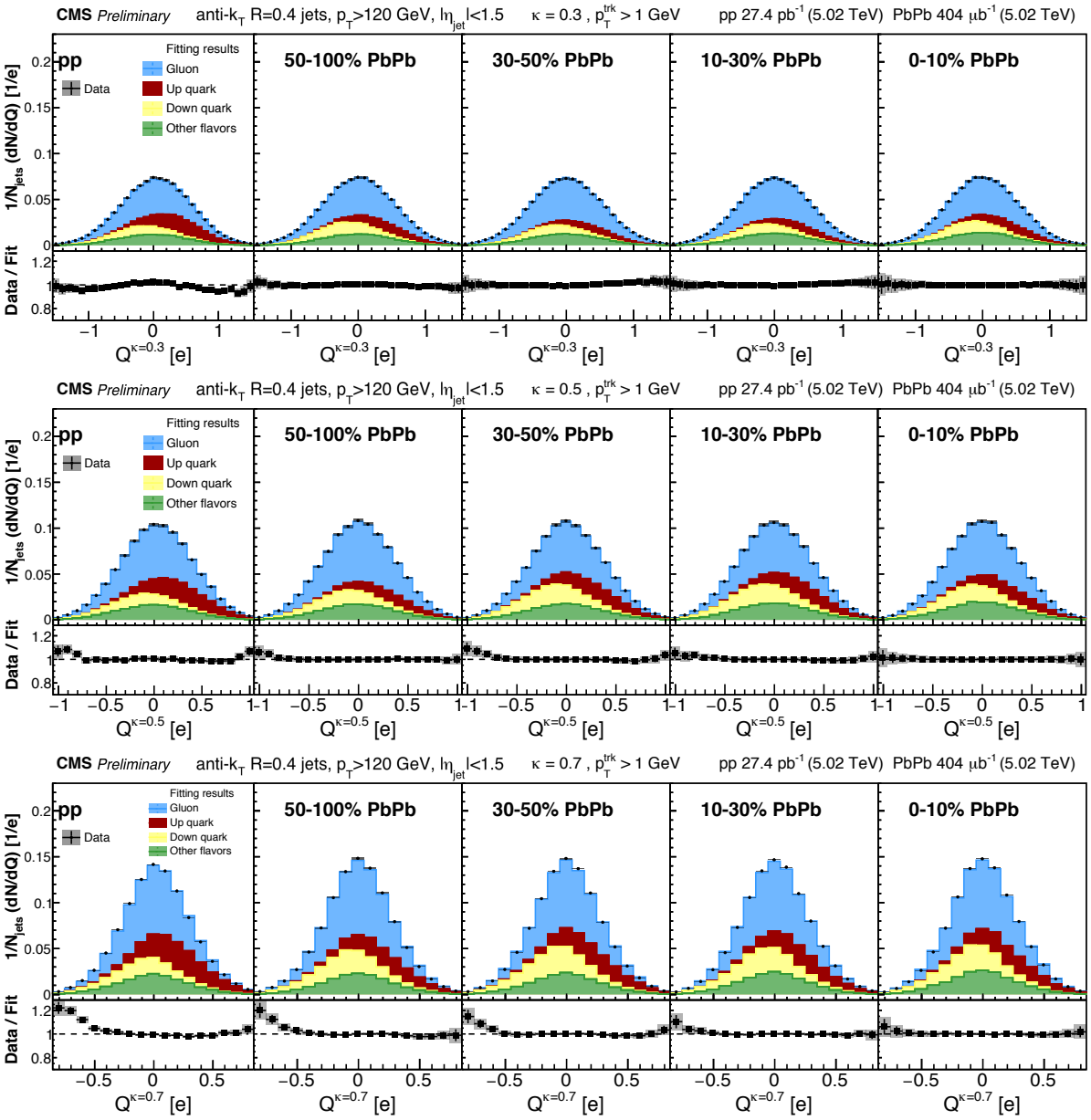

Figure 6: (Top) Unfolded jet charge measurements shown for inclusive jets in data along with the extracted fractions of up and down quark jets, gluon jets, and the heavy and antiquark jets (collectively grouped as "other flavors"). The systematic uncertainties on the distributions are shown in shaded regions around the measurements. The jet charge measurements shown here are for $\kappa = 0.3$, $\kappa = 0.5$ and $\kappa = 0.7$ and a minimum track p_{T} of 1 GeV. (Bottom) Ratio of the jet charge measurements to the results of template fits.

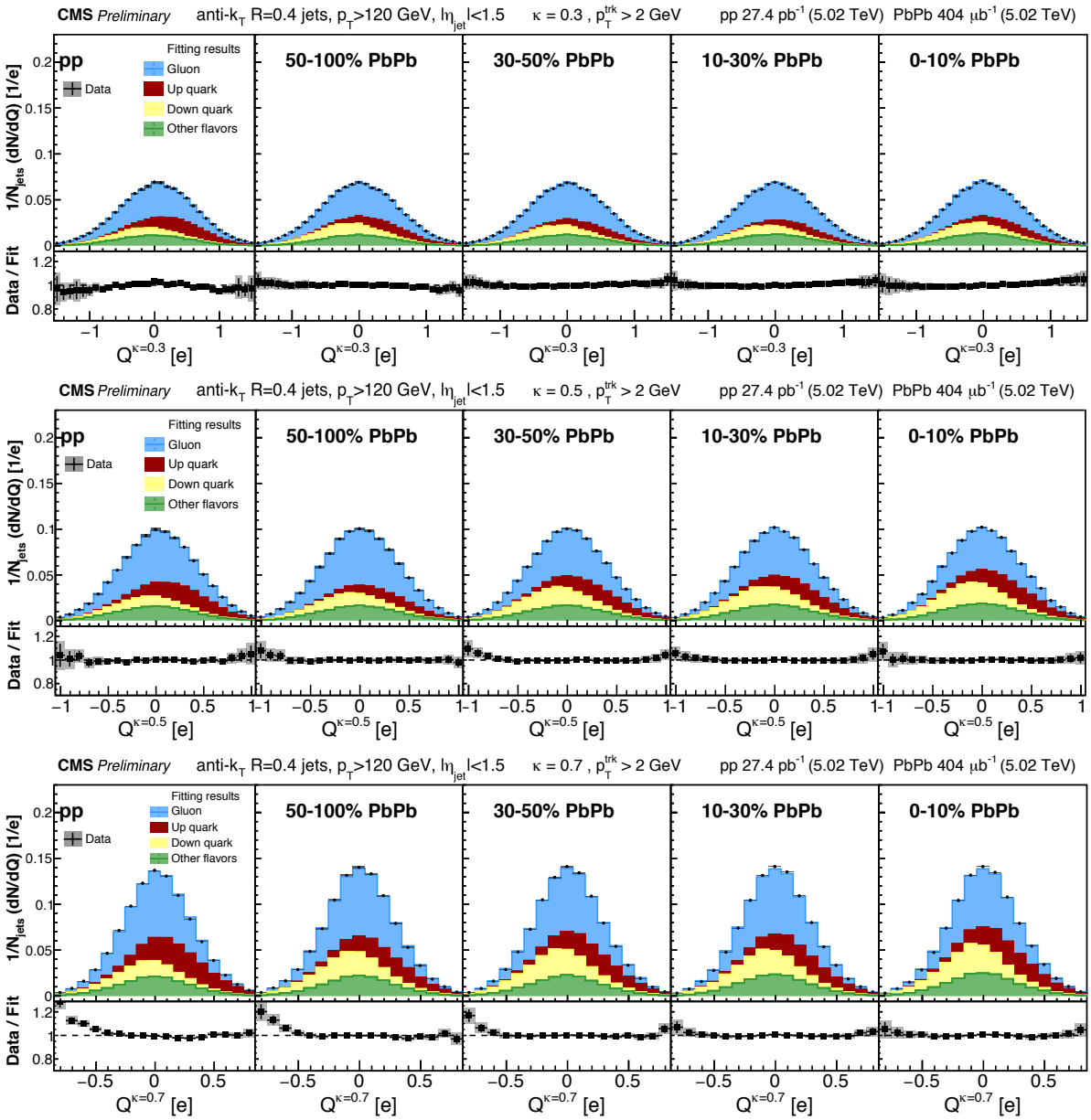

Figure 7: (Top) Unfolded jet charge measurements shown for inclusive jets in data along with the extracted fractions of up and down quark jets, gluon jets, and the heavy and antiquark jets (collectively grouped as "other flavors"). The systematic uncertainties on the distributions are shown in shaded regions around the measurements. The jet charge measurements shown here are for $\kappa = 0.3$, $\kappa = 0.5$ and $\kappa = 0.7$ and a minimum track p_{T} of 2 GeV. (Bottom) Ratio of the jet charge measurements to the results of template fits.